Detection of 2-Hydroxyglutarate in IDH-mutated Glioma Patients by Spectral-editing and 2D Correlation Magnetic Resonance Spectroscopy

Ovidiu C. Andronesi[1,*], **Grace Kim**[1], **Elizabeth Gerstner**[2], **Tracy Batchelor**[2], **Aria A. Tzika**[3], **Valeria R. Fantin**[4], **Matthew G. Vander Heiden**[5], and **A. Gregory Sorensen**[1]

[1]Athinoula A. Martinos Center for Biomedical Imaging, Department of Radiology, Massachusetts General Hospital, Harvard Medical School, Boston, MA 02114, USA

[2]Pappas Center for Neuro-Oncology, Massachusetts General Hospital, Harvard Medical School, Boston, MA 02114, USA

[3]NMR Surgical Laboratory, Department of Surgery, Massachusetts General Hospital and Shriners Burn Institute, Harvard Medical School, Boston, MA 02114, USA

[4]Agios Pharmaceuticals, Cambridge, MA 02139, USA

[5]Koch Institute for Integrative Cancer Research, Massachusetts Institute of Technology, Cambridge, MA 02139, USA

Abstract

Mutations of arginine 132 (R132) in the enzyme isocitrate dehydrogenase-1 (IDH1) are present in up to 86% of grade II and III gliomas and secondary glioblastoma. R132 mutations in IDH1 result in excess production of the metabolite 2-hydroxyglutarate (2HG), which could be used as a biomarker for this subset of gliomas. Here, we use optimized spectral-editing and two-dimensional (2D) correlation magnetic resonance spectroscopy (MRS) methods to unambiguously detect 2HG non-invasively in glioma patients with IDH1 mutations. By comparison, fitting of conventional 1D MR spectra can provide false-positive readouts owing to spectral overlap of 2HG and chemically similar brain metabolites, such as glutamate and glutamine. 2HG has been found also by 2D high-resolution magic angle spinning MRS performed ex vivo on a separate set of glioma biopsy samples. 2HG detection by in vivo or ex vivo MRS enabled detailed molecular characterization of a clinically important subset of human gliomas. This has implications for diagnosis as well as monitoring of treatments targeting IDH mutations.

INTRODUCTION

Isocitrate degydrogenase 1 (IDH1) is an intracellular enzyme that catalyzes the oxidative decarboxylation of isocitrate to α-ketoglutarate in the cytoplasm and in peroxisomes. Recent genomic studies have identified heterozygous point mutations in arginine 132 (R132) of the IDH1 enzyme (1, 2). These mutations result in a neomorphic activity leading to

---

*To whom correspondence should be addressed. ovidiu@nmr.mgh.harvard.edu.

Competing interests: O.C.A. and A.G.S have applied for a patent for the 2D COSY-LASER method that is used in the paper.

overproduction and accumulation of the *R* (also D) enantiomer of the metabolite 2-hydroxglutarate (2HG) in 68 to 86% of grade II-III astrocytic and oligodendroglial tumors, as well as grade IV secondary glioblastoma, having higher frequency in young patients (3-5). Glioma patients with *IDH1* mutations have a greater 5-year survival rate than patients with wild-type *IDH1* gliomas (93% versus 51%) when correcting for age (3), suggesting that *IDH1* mutations represent a clinically distinct subset of patients. In addition to glioma, mutations in *IDH1* have also been found in patients with acute myelogenous leukemia and various other tumors, but at lower frequency than in glioma (6).

The full impact of the R132 mutation is not yet fully understood, but a major consequence of mutating this residue in IDH1 is a gain-of-function enzymatic activity favoring reduction of α-ketoglutarate to 2HG (7). This neomorphic activity leads to the accumulation of 2HG, a metabolite usually present in low levels in vivo as an error product of normal metabolism. Analogous mutations in the mitochondrial IDH2 isoform also result in 2HG production, but *IDH2* mutations are found less frequently than *IDH1* in various tumors, including gliomas (4).

2HG is a small biomolecule that has been shown ex vivo to identify *IDH1/2*-mutant tumors in humans (8). In transfected U87MG glioblastoma cell cultures, the intracellular concentration of 2HG can increase over 100-fold (7), up to 5-35 µmol/g (or 5-35 mM, assuming tissue density of 1.05 g/ml), after introduction of R132 mutated IDH1 in the U87MG genome. Accumulation of 2HG to similar levels as in U87MG cell cultures was measured in human glioma biopsy samples with $IDH1_{R132}$ mutations (7, 9). This high concentration of 2HG (5-35 mM) is suitable for detection by in vivo magnetic resonance spectroscopy (MRS). Because the sensitivity threshold of in vivo MRS is roughly 1 mM, 2HG is not expected to be visible under normal conditions; but, 2HG might become measurable upon local accumulation owing to *IDH* mutation. Thus, the presence or absence of 2HG in the MR spectrum of glioma patients could effectively genotype tumors as being positive or negative for *IDH1* or *IDH2* mutations.

The *S* (also L) enantiomer of 2HG (L-2HG) has been detected using MRS in vivo in patients with hydroxyglutaric aciduria (10, 11). The detection challenge arises from the fact that the 2HG spectrum is largely overlapping with glutamate (Glu) and glutamine (Gln) — both abundant brain metabolites that have a similar five-spin system. Peaks in the region of 2.6 to 2.4 ppm that were previously indicated (10, 11) for L-2HG are shared with Glu, Gln, and also by *N*-acetyl-L-aspartate (NAA). With the limited in vivo spectral resolution (0.1 ppm) present in most clinical settings, these overlapping species are not easily resolved using conventional one-dimensional (1D) MRS, especially if spectral fitting was not used, as in these earlier reports (10, 11). Spectral fitting programs (12, 13) try to model the in vivo MR spectrum as a combination of modeled spectra (basis set) from all detectable metabolites. This approach might fail at clinically available fields when there is severe overlap as it is well known for GABA (14), or as we show in this paper for 2HG.

Two-dimensional (2D) correlation spectroscopy (COSY) (15) can potentially differentiate the overlapping metabolite spectra, because correlating two chemical shifts of coupled spins creates specific patterns of signals (crosspeaks) for each metabolite that are better separated in the plane of the 2D spectrum than spectral lines in a 1D spectrum. The 2D COSY exploits the idea that there is less likelihood for two metabolites to have two identical shifts, even if they might share a common chemical shift in the 1D spectrum. In particular, the crosspeaks involving H_α protons of 2HG appears in a region of the 2D COSY spectra where no other metabolite is found in healthy tissue or tumors without *IDH* mutations. Hence, although in 1D spectra the signals of 2HG appear in a region where other metabolites normally contribute, in 2D COSY spectra the crosspeaks involving H_α protons of 2HG can be

uniquely identified. Alternatively, spectral-editing of 1D MRS, such as J-difference spectroscopy (14), can be tuned to detect a specific metabolite by removing the contribution of unwanted overlapping metabolites. The spectral-editing experiment can be easier to run on clinical scanners but offers limited metabolite information, while on the other hand the 2D COSY retains the full spectral information at the expense of complexity of the experiment.

In this work, we show that 2HG can be detected unambiguously in glioma patients using an optimized in vivo adiabatic 2D COSY method, developed previously for studying brain metabolism (16), or by spectral-editing MRS. We also find that fitting conventional 1D spectra might provide false positive results. In vivo measurements were compared with ex vivo high resolution magic angle spinning (HR-MAS) 2D MRS and liquid chromatography-mass spectrometry (LC-MS) of glioma biopsy samples. Results from brain phantoms, two glioma patients harboring the *IDH1* R132 mutation, and eight control cases, including primary glioblastoma (n = 4) and healthy volunteers (n = 4) with wild-type *IDH1*, demonstrate that non-invasive detection of 2HG using 1D spectral-editing and 2D correlation MRS is feasible and may allow stratification of patients on the basis of *IDH1* mutation.

RESULTS

Spectroscopic detection of 2HG in phantoms

We performed phantom experiments at 3T on clinical scanners to establish that 2HG can be distinguished from other metabolites by localized 2D correlation MRS as well as localized spectral-editing 1D MRS. 2HG was added to a phantom containing a mixture of brain metabolites, and a recently developed 2D LASER-COSY sequence (16) with improved in vivo performance based on localized adiabatic selective refocusing (LASER) was used as described in Methods. An adiabatic spectral-editing sequence (MEGA-LASER) was newly designed in this paper specifically for the purpose of 2HG detection (Methods and supplementary figs. S1, S3). A series of phantoms with a range of 2HG concentrations expected to be present in IDH-mutant tumors were also investigated to test the sensitivity limit of MRS. Assignments of 2HG (17) and other metabolites, such as myo-inositol (Myo), choline (Cho), *N*-acetylaspartic acid (NAA), glutamate (Glu), glutamine (Gln), and γ-amino-butyric acid GABA were made (Fig. 1) according to published literature values (18).

Fig. 1A shows the overlay of 2D LASER-COSY spectra recorded in a phantom containing a mixture of 2HG and brain metabolites (blue contours), and a phantom that contains only normal brain metabolites (red contours). The normal brain metabolites are at physiological concentrations in both phantoms. The H_α-H_β crosspeak of 2HG located at 4.02/1.91 (δ_2/δ_1) ppm is well-separated from other metabolites, including the chemically similar metabolite glutamate, with H_α-H_β correlation located at 3.75/2.12 ppm. Detailed information of the overlap between 2HG and other metabolites can be gleaned from spectra simulations (fig. S2). The strongly coupled five-spin system of 2HG, Glu, and Gln are very similar, and a large overlap is observed in the 2.6-2.0 ppm region for H_β and H_γ protons. Additionally, GABA overlaps 2HG between 2.0-1.8 ppm and 2.4-2.2 ppm. As expected from the chemical structure, the largest separation between 2HG, Glu, and Gln is noticed for H_α protons owing to attached hydroxyl and amino moieties at C_α on 2HG and Glu/Gln, respectively. This H_α separation can be exploited in spectral-editing MRS.

Fig. 1B shows the edited 1D spectra obtained with the MEGA-LASER sequence on the same phantom as Fig. 1A. The H_α multiplet signal of 2HG at 4.02 ppm (Fig. 1B, blue) is aligned with the 2HG crosspeak from the 2D LASER-COSY spectrum. The signal at 4.02 ppm is missing in the brain phantom that does not contain 2HG (Fig. 1B, red). In addition to

2HG, the multiplet signals of Glu at 3.75 ppm and GABA at 3.01 ppm are co-edited, and their multiplets can be better observed in the inset of Fig. 1B. By comparison, in conventional 1D spectra obtained with LASER, the H_α proton of 2HG is largely overlapped by the strong H_β peak of myo-inositol at 4.05 ppm (fig. S2). For in vivo spectroscopy, which typically has lower spectral resolution owing to susceptibility anisotropy of tissues, the H_α proton of 2HG might be obscured more even by the neighboring peaks of lactate (4.09 ppm) and both creatine and phosphocreatine (3.91 ppm).

MEGA-LASER showed excellent localization when compared to MEGA-PRESS in fig. S3, with no contamination of lipid signal from outside the voxel. The echo time of MEGA-LASER was optimized around the value of 1/2J (J, scalar coupling) for maximizing H_α signal of 2HG. The maximum was found for TE = 75 ms.

Calibration measurements were made for a series of 2HG phantoms with concentrations in the range of 0 to 16 mM (Fig. 1C). A strong correlation ($R = 0.992$) was found between 2D LASER-COSY crosspeak volume and 2HG concentration. A sensitivity limit of 2 mM 2HG was calculated for 2D LASER-COSY, with a voxel of 27 cm^3, measurement time of 12.8 min, and a minimum signal-to-noise ratio (SNR) of 5, for reliable identification of the H_α crosspeaks. Similar strong correlation ($R = 0.995$) was found between 2HG concentration and the area of 2HG peak in spectral-editing MEGA-LASER. The SNR of 5 for 2 mM 2HG concentration and 27 cm^3 voxel can be reached by MEGA-LASER with a shorter acquisition time of 5 min..

2HG detection in intact brain biopsies

To ensure that 2HG measurements were possible in human tissue, we measured brain biopsy samples ($n = 10$, Table 1) prior to in vivo experiments. Biopsies were used because they contain the full set of metabolites and tumor metabolic profiles that are hard to replicate in phantoms. 2D spectra were obtained with HR-MAS conditions at 14 T from brain biopsies representing varied pathologies and *IDH1* mutation status (Fig. 2). The ^{1}H-^{1}H 2D TOBSY [Total Through Bond Spectroscopy (18)] spectra of an *IDH1*-mutated anaplastic astrocytoma contained well-resolved and separated 2HG crosspeaks involving the correlations of H_α with H_β (4.02/1.91 ppm) and H_γ (4.02/2.24 ppm) (Fig. 2A). The 2HG crosspeaks from biopsy spectrum overlaid entirely with the corresponding 2HG crosspeaks of the phantom spectrum (Fig. 2A). Projections along δ_1 and δ_2 spectral dimensions through the 2HG crosspeaks of the anaplastic astrocytoma biopsy are shown along axes of the 2D TOBSY. Importantly, 2HG signals are not present in the 2D TOBSY spectra from both primary glioblastoma (Fig. 2B) and non-tumor control (Fig. 2C) tissues, which were both wild-type *IDH1*. Of notice though, our 2HG findings from HRMAS measurements are based on the single biopsy that had mutant *IDH1*.

In addition to 2HG, large qualitative and quantitative differences are easily observed among different biopsy samples; most notably the presence of lipids, L-fucose, and β-glucose, as well as the absence of glutathione (GSH) in glioblastoma; the increased GPC (glycerophosphocholine) to PC (phosphocholine) ratio in anaplastic astrocytoma compared to non-tumor control biopsy; and a decreased GPC to PC ratio in glioblastoma compared to non-tumor control biopsy (Fig. 2). Similar finding have been previously reported, regarding increased lipids (19) and the presence of L-fucose in glioblastoma (20), and increased GPC in low grade glioma versus increased PC in high grade glioma (21-23). For comparison, 1D HRMAS spectra acquired on the anaplastic astrocytoma biopsy are shown in fig. S4. Because no tissue is destroyed during HR-MAS measurements, further assays are possible, such as histology, genomics, or mass spectrometry, to fully characterize the tumors. LC-MS was performed on the same biopsies and 2HG levels were measured to be 151.58 ng 2HG per mg tissue (wet weight) for *IDH1*$_{R132H}$ anaplastic astrocytoma, 2.39 ng/mg for wt-*IDH1*

glioblastoma, and 1.79 ng/mg for wt-*IDH1* non-tumor control. The 2HG level in *IDH1*$_{R132H}$ anaplastic astrocytoma was 1.02 µmol/g-tissue, which is an order of magnitude above the 0.1 µmol/g lower sensitivity limit of HR-MAS (24); whereas the wt-IDH1 tissues had almost 100-fold less 2HG (0.01-0.015 µmol/g), concordant with previous results (7). The 2HG levels in wt-*IDH1* biopsies are <0.1 µmol/g (detection threshold of HR-MAS) and hence not visible in Fig. 2, B and C.

In vivo 2HG detection by spectral-editing and 2D correlation MRS

After confirming MRS detection of 2HG in biopsy tissue ex vivo, MRS spectroscopy was performed in vivo in a separate set of human subjects (*n* = 10, Table 2). The results obtained on biopsies were important to identify the 2HG peaks that have the best chances to be detected in vivo and helped us select the appropriate in vivo methods. Two glioma patients (*n* = 2) with known *IDH1* mutations (R132C and R132H), as well as two control groups, including primary glioblastoma patients without *IDH1* mutations (*n* = 4) and healthy, non-tumor volunteers (*n* = 4) were investigated. Single voxels were prescribed based on fluid attenuation inversion recovery (FLAIR) image abnormalities in tumor patients, and magnetization prepared by rapid acquisition of gradient echo (MEMPRAGE) images in volunteers. 2D LASER-COSY, 1D MEGA-LASER, and 1D LASER spectra were acquired from the tumor patients and volunteers.

2D LASER-COSY results from a patient with anaplastic astrocytoma confirmed by tumor DNA sequencing to have R132C mutation of IDH1 are shown in Fig. 3A. A 27 cm^3 voxel (3×3×3 cm^3) was placed on the FLAIR images to include most of the solid tumor located in the splenium of the corpus callosum and the tail of the left hippocampus. The H$_\alpha$-H$_\beta$ crosspeak of 2HG was present in the 2D LASER-COSY spectrum at 4.02/1.91 ppm (δ_2/δ_1), with δ_2 and δ_1 projections well above the baseline noise level (Fig. 3A). Similar 2HG projections can be observed in the phantom spectrum (fig. S2A). Crosspeaks of several other metabolites can be identified (Fig. 3A). Results from LCModel fitting of 1D LASER spectra are shown in fig. S5. Considering a basis set of spectra formed by the 20 most abundant metabolites in addition to 2HG, the fitting algorithm estimated the contribution of each metabolite so that the computed spectrum overlaps as best as possible with the measured spectrum (fig. S5).

An example of 2D LASER-COSY from a primary glioblastoma patient (wt-IDH1 by tumor DNA sequencing) is shown (Fig. 3B). A slightly bigger voxel (3.5×3.5×3.5 cm^3) was chosen owing to the extension of the tumor into the left occipital lobe. The 2D LASER-COSY does not contain any 2HG crosspeak in the H$_\alpha$ region outlined by the green rectangle. Fitting methods applied to conventional 1D MRS (fig. S6) erroneously suggest the large presence of 2HG within confidence limits for goodness of fit (16% Cramer-Rao bounds), and that the level of 2HG is higher than NAA or GPC. These latter metabolites are both present in the 2D LASER-COSY spectrum; therefore, if the computed 1D MRS results in fig. S6 were true, the 2HG should be also visible in the 2D spectrum in Fig. 3B. This contradiction suggests that, in this case, the fitted 1D MRS result represents a false-positive. Fitting programs, such as LCModel, assume that the composite spectrum can be obtained by a unique combination of individual metabolite spectra. However, this is known to fail for in vivo spectra due to adverse combination of lower resolution and severe overlap of weaker metabolite signals by stronger metabolite signals. The most known example is erroneous GABA measurement by fitting conventional 1D spectra (25). On the other hand, 2D LASER-COSY is more in line with the genetic analysis that showed no *IDH1* mutations in this patient.

Fig. 3C shows data from a healthy volunteer with wild-type *IDH1*. A 27 cm^3 voxel was placed in the white matter of the left occipital lobe similar to the patient tumor positions.

2HG is absent, as expected, from the 2D LASER-COSY spectrum with the H_α crosspeak region outlined in green. 2D spectral quality is indicated by projections through the glutamate and glutamine crosspeak (Glu+Gln, 3.75/2.12 ppm). The fitting of the 1D MRS from the healthy volunteer is shown in fig. S7. The Cramer-Rao lower bound (23%) for 2HG fit is only slightly above the accepted limit (20%) for goodness of fit. However, 2HG was not expected to be found in a healthy control (see fig. S9 where the LCModel fits 2HG with 17% Cramer-Rao bounds in the healthy contralateral hemisphere of the glioblastoma patient).

Results obtained with the spectral-editing 1D MEGA-LASER sequence are presented in Fig. 4. Overlay of spectra acquired from tumor and the healthy contralateral side in a secondary glioblastoma patient with $IDH1_{R132H}$ mutation is shown in Fig. 4A. Importantly, the H_α multiplet signal of 2HG around 4.02 ppm is found only in the tumor spectrum and not on the healthy side. The multiplets of glutamate and glutamine (Glu+Gln), and GABA [+macromolecules (MM)] are present in both voxels. LCModel fitting of the corresponding non-edited 1D LASER spectra showed 2HG in tumor (Cramer-Rao 15%) (fig. S8) and also in the healthy voxel (Cramer-Rao 17%) (fig. S9), contrary to expectations.

Spectra from the control primary glioblastoma patient (wt-*IDH1*) (Fig. 4B) and from the healthy volunteer (wt-*IDH1*) (Fig. 4C) do not contain any 2HG; but they do show Glu+Gln and GABA+MM peaks. Interestingly, the Glu+Gln peaks in tumor voxels seem to be shifted slightly upfield compared to healthy side spectra (Fig. 4, A and B). The shift can be caused by different pH conditions in tumors compared to healthy brain tissue, and by different Glu and Gln relative contributions. There is no shift for Glu+Gln peaks between right and left sides in the healthy volunteer (Fig. 4C). No shift was observed for the GABA+MM peaks in any subject (Fig. 4).

Quantification of 2HG from in vivo spectral-editing and 2D correlation MRS

Quantitative analysis of 2D LASER-COSY, 1D MEGA-LASER, and 1D LASER spectra was performed using the ratio of 2HG to the sum of Glu+Gln for reasons outlined in Methods. Volumes of crosspeaks at 4.02/1.91 ppm for 2HG and 3.75/2.12 ppm for Glu+Gln were used to calculate the 2HG/(Glu+Gln) ratio from 2D LASER-COSY (Fig. 5A). Areas of peaks at 4.02 ppm for 2HG and 3.75 ppm for Glu+Gln were used to estimate the 2HG/(Gln +Glu) ratio from 1D MEGA-LASER (Fig. 5B). For 1D LASER, the values fitted by LCModel (Fig. 5, A and B) were used to calculate the ratio.

The 2HG/(Glu+Gln) ratios are plotted for phantoms ($n = 2$), mutant $IDH1_{R132H}$ glioma patients ($n = 2$), wt-*IDH1* glioblastoma patients ($n = 4$), and healthy volunteers ($n = 4$) (Fig. 5). In the case of phantoms, there is very good agreement between 2D correlation (LASER-COSY) MRS, 1D spectral-editing (MEGA-LASR) MRS, and 1D conventional (LASER) MRS for the 2HG/(Glu+Gln) ratio, which was close to 0.4, as expected from their respective concentrations: 2HG (3 mM), Glu (7.5 mM), Gln (0 mM). Because of similar spin systems, the ratio of crosspeak volumes was determined by their concentrations (assuming similar T_2 and T_1 times), without the need to correct for number of protons and build-up rates.

In the case of mutant R132-IDH1 glioma patients estimation of 2HG/(Glu+Gln) ratio showed slight differences which, however, are not statistical significant (P = 0.28). 2D LASER-COSY and 1D MEGA-LASER found an average ratio of 1.27, whereas LCModel fitting estimated an average ratio of 1.11 (Fig. 5). In the wt-IDH1 primary glioblastoma and non-tumor controls there was significant difference (P = 0.03) between the 2HG/(Glu+Gln) ratios obtained by LCModel fitting (ratios 0.33 and 0.57), and 2D LASER-COSY (ratio 0.04) and 1D MEGA-LASER (ratio 0.03), respectively.

DISCUSSION

The discovery that mutated *IDH1/2* in gliomas can be correlated with survival benefit (3) has generated interest in using this mutation for diagnostic and prognostic purposes. 2HG is a metabolite that accumulates in human gliomas that harbor *IDH1* mutations. Here, we preliminarily show that 2HG can be detected unambiguously and non-invasively by localized 2D correlation and 1D spectral-editing MRS in patients with mutated *IDH1*.

In vivo MRS detection of 2HG in gliomas has been suggested previously (7). Our results show that 2D LASER-COSY and 1D MEGA-LASER can reliably identify 2HG. The sensitivity of 2D LASER-COSY was approximately 2 mM (or 10 mg) for a $3\times3\times3$ cm^3 voxel, using a 13-min in vivo acquisition time and a minimum SNR of 5. The same sensitivity can be achieved by 1D MEGA-LASER in 5-min scan for the same voxel size. This is sufficient for the range (5 to 35 mM) of 2HG concentrations reported in *IDH1*-mutant tumors. Although the voxels used seem to be pretty large, several aspects besides maximizing sensitivity may justify this choice. First, gliomas are very infiltrative tumors with ill-defined margins, and active tumor exceeds the contours of the T_1-weighted post-contrast images, which are mostly used to report tumor diameters or volumes. Second, *IDH1* mutations seem to be uniformly expressed in tumors when present (26), so a large tumor volume could be included in the voxel. Finally, our method can separate or remove the contribution of normal metabolite; hence the inclusion of healthy tissue, which we showed does not contain 2HG, does not alter 2HG estimation. Further improvements in spatial resolution and multivoxel acquisitions of 2D LASER-COSY (27) or spectral-editing MRS (28) are possible. In addition, the sensitivity of ex vivo HRMAS approaches 1 μM and may therefore be employed as a non-destructive method for more detailed metabolite profiling in tumor samples.

Relative quantification of in vivo MRS data indicated that a 2HG/(Glu+Gln) ratio >1 could be specific for *IDH1* mutations. Moreover, existing data indicate that 2HG and Glu might be inversely proportional: a slight decrease of Glu together with a large increase of 2HG in *IDH1*$_{R132H}$ (9), compared with a slight increase of Glu (20) with virtually undetectable 2HG (7) in wild-type *IDH1* gliomas. These results suggests that the 2HG/(Glu+Gln) ratio might have increased dynamic range for detecting *IDH1* mutations compared with either metabolite alone.

Comparing 2D correlation and 1D spectral-editing MRS, each method has its own strengths and limitations. For example, all metabolites are preserved and identified by two well-defined chemical shifts in 2D COSY, whereas in 1D spectral-editing, there is only one well-defined chemical shift in addition to a range of possible chemical shifts given by the bandwidth of the selective pulse (fig. S1). Conversely, spectral-editing experiments are easier to run and may require shorter scan times or smaller voxel sizes to detect the same concentration.

In addition to using 2HG as a biomarker, there is mounting interest in deciphering the biological mechanisms that link *IDH* mutations, 2HG production, and tumorigenesis. 2HG might act as an oncometabolite by competitive inhibition of α-ketoglutarate–dependent dioxygenases (29). This includes inhibition of histone demethylases and 5-methlycytosine (5 mC) hydroxylases, leading to genome-wide alterations in histone and DNA methylation, as well as inhibition of hydroxylases resulting in up-regulation of hypoxia-inducible factor 1 (HIF-1) (30). Hence, a large interest exists from pharmacological companies and research groups to develop inhibitors of mutated *IDH1*$_{R132}$. The ability to objectively and non-invasively follow the effects of these compounds in animals and patients is a pre-requisite for successful drug development.

The importance of a reliable method for a novel noninvasive method of detecting 2HG in vivo is underscored by the fact that no report exists about increased D-2HG in the blood, cerebrospinal fluid, or urine of glioma patients with *IDH1* mutations. This situation is different from hydroxyglutaric aciduria metabolic disorders, which show high levels of L-2HG in body fluids. Therefore, other than tumor biopsy, no assay currently exists to probe 2HG in *IDH*-mutated gliomas. Although a biopsy might be necessary for the initial diagnosis, multiple serial brain biopsies are generally not feasible. Moreover, MRS methods could map 2HG distribution and identify 2HG hot spots, guiding biopsy procedures to increase the chances for correct typing of the tumor, since it is known that biopsy based on conventional CT or MRI is suboptimal and subject to undergrading (31).

The in vivo 2D correlation and 1D spectral-editing MRS methods that we demonstrated can be repeated noninvasively, without harmful effects to patients, and might facilitate preclinical or clinical studies of new therapies, as well as assist with initial diagnostic workup. With further validation in humans, this approach could even allow molecular typing of *IDH*-mutant tumor using magnetic resonance imaging (MRI) investigations, which are already included in most patients' diagnostic work-up, resulting in cost-effective and rapid genotyping of *IDH* mutations.

MATERIALS and METHODS

Complete details for all the methods are given in the Supplementary Material.

Selection of human subjects

Patients and healthy volunteers (*n = 10* total) listed in Table 2 were scanned with informed consent approved by the Internal Review Board at Massachusetts General Hospital.

Biopsy collection for HRMAS and LC-MS

Biopsies (*n*= 10, Table 1) were collected at the time of surgery and snap frozen in liquid nitrogen.

Genetic analysis for *IDH1* mutation

A multiplexed allele-specific assay (32) was used to detect somatic mutations in tumor DNA extracted from formalin-fixed paraffin-embedded samples.

Brain phantoms

Two phantoms with a mixture of metabolites were prepared for the initial assessment of unambiguous 2HG detection with MRS. One phantom contained normal brain metabolites at physiological concentrations. Another phantom contained the same brain metabolites as the first phantom, but also had 3 mM of D-2HG (D-α-hydroxyglutaric acid disodium salt, Sigma Aldrich). A series of phantoms containing only 2HG at different concentrations were prepared for calibration and sensitivity tests.

Simulations of metabolite spectra

Quantum mechanical simulations were done in GAMMA [General Approach To Magnetic Resonance Mathematical Analysis (33)] for spectra of 2HG and the overlapping brain metabolites Glu, Gln, and GABA.

Ex vivo HR-MAS NMR spectroscopy

All HR-MAS experiments were conducted on a wide-bore 14.1 T (600 MHz ^{1}H) Bruker Avance spectrometer using a 4 mm double channel HR-MAS probehead (Bruker). 2D spectra were measured at 3 kHz MAS using a 2D TOBSY (20) sequence.

LC-MS of brain biopsies

The same biopsies measured by HRMAS were used for LC-MS metabolic profiling (7). Eluted metabolite ions were detected using a triple-quadrupole mass spectrometer, tuned to detect eight known central metabolites, including 2-HG.

Acquisition of in vivo MR spectroscopy

All in vivo MR scans were performed on 3 T Tim Trio scanners (Siemens, Erlangen), using a head 32-channel phased array for receive and body radio-frequency (RF) coil for transmit. Single voxel spectroscopy was performed using recently optimized 1D LASER (34) and the 2D LASER-COSY (16) sequences. In addition, a newly designed 1D MEGA-LASER was used for spectral-editing (fig. S1). Typical voxel sizes were 27 cm^3 (3×3×3 cm^3) or 42.8 cm^3 (3.5×3.5×3.5 cm^3), in case of large tumors. A repetition time (TR) of 1.5s was used for all acquisitions. For 1D LASER and 2D LASER-COSY an echo time (TE) of 45 ms was used. The 1D MEGA-LASER spectra were acquired with TE of 75 ms.

Processing, analysis, and quantification of in vivo MR spectroscopy

Raw data were exported from the Siemens scanners for subsequent processing and analysis. The 1D LASER data (FID) were processed and quantified with LCModel (12) using a GAMMA-simulated basis set for LASER. For 1D MEGA-LASER data fitting was done in jMRUI (13). For 2D LASER-COSY, the FIDs of all t1 increments were imported in Matlab (The Mathworks) and futher processed. For quantification and comparison of methods and subjects, the 2HG/(Glu+Gln) ratio was chosen.

Supplementary Material

Refer to Web version on PubMed Central for supplementary material.

Acknowledgments

REFERENCES AND NOTES

1. Parsons DW, Jones S, Zhang XS, Lin JCH, Leary RJ, Angenendt P, Mankoo P, Carter H, Siu IM, Gallia GL, Olivi A, McLendon R, Rasheed BA, Keir S, Nikolskaya T, Nikolsky Y, Busam DA, Tekleab H, Diaz LA, Hartigan J, Smith DR, Strausberg RL, Marie SKN, Shinjo SMO, Yan H, Riggins GJ, Bigner DD, Karchin R, Papadopoulos N, Parmigiani G, Vogelstein B, Velculescu VE, Kinzler KW. Science. Sep.2008 321:1807. [PubMed: 18772396]

2. Chin L, Meyerson M, Aldape K, Bigner D, Mikkelsen T, VandenBerg S, Kahn A, Penny R, Ferguson ML, Gerhard DS, Getz G, Brennan C, Taylor BS, Winckler W, Park P, Ladanyi M, Hoadley KA, Verhaak RGW, Hayes DN, Spellman PT, Absher D, Weir BA, Ding L, Wheeler D, Lawrence MS, Cibulskis K, Mardis E, Zhang JH, Wilson RK, Donehower L, Wheeler DA, Purdom E, Wallis J, Laird PW, Herman JG, Schuebel KE, Weisenberger DJ, Baylin SB, Schultz N, Yao J, Wiedemeyer R, Weinstein J, Sander C, Gibbs RA, Gray J, Kucherlapati R, Lander ES, Myers RM, Perou CM, McLendon R, Friedman A, Van Meir EG, Brat DJ, Mastrogianakis GM, Olson JJ, Lehman N, Yung WKA, Bogler O, Berger M, Prados M, Muzny D, Morgan M, Scherer S, Sabo A,

Nazareth L, Lewis L, Hall O, Zhu YM, Ren YR, Alvi O, Yao JQ, Hawes A, Jhangiani S, Fowler G, San Lucas A, Kovar C, Cree A, Dinh H, Santibanez J, Joshi V, Gonzalez-Garay ML, Miller CA, Milosavljevic A, Sougnez C, Fennell T, Mahan S, Wilkinson J, Ziaugra L, Onofrio R, Bloom T, Nicol R, Ardlie K, Baldwin J, Gabriel S, Fulton RS, McLellan MD, Larson DE, Shi XQ, Abbott R, Fulton L, Chen K, Koboldt DC, Wendl MC, Meyer R, Tang YZ, Lin L, Osborne JR, Dunford-Shore BH, Miner TL, Delehaunty K, Markovic C, Swift G, Courtney W, Pohl C, Abbott S, Hawkins A, Leong S, Haipek C, Schmidt H, Wiechert M, Vickery T, Scott S, Dooling DJ, Chinwalla A, Weinstock GM, O'Kelly M, Robinson J, Alexe G, Beroukhim R, Carter S, Chiang D, Gould J, Gupta S, Korn J, Mermel C, Mesirov J, Monti S, Nguyen H, Parkin M, Reich M, Stransky N, Garraway L, Golub T, Protopopov A, Perna I, Aronson S, Sathiamoorthy N, Ren G, Kim H, Kong SK, Xiao YH, Kohane IS, Seidman J, Cope L, Pan F, Van Den Berg D, Van Neste L, Yi JM, Li JZ, Southwick A, Brady S, Aggarwal A, Chung T, Sherlock G, Brooks JD, Jakkula LR, Lapuk AV, Marr H, Dorton S, Choi YG, Han J, Ray A, Wang V, Durinck S, Robinson M, Wang NJ, Vranizan K, Peng V, Van Name E, Fontenay GV, Ngai J, Conboy JG, Parvin B, Feiler HS, Speed TP, Socci ND, Olshen A, Lash A, Reva B, Antipin Y, Stukalov A, Gross B, Cerami E, Wang WQ, Qin LX, Seshan VE, Villafania L, Cavatore M, Borsu L, Viale A, Gerald W, Topal MD, Qi Y, Balu S, Shi Y, Wu G, Bittner M, Shelton T, Lenkiewicz E, Morris S, Beasley D, Sanders S, Sfeir R, Chen J, Nassau D, Feng L, Hickey E, Schaefer C, Madhavan S, Buetow K, Barker A, Vockley J, Compton C, Vaught J, Fielding P, Collins F, Good P, Guyer M, Ozenberger B, Peterson J, Thomson E. Nature. Oct.2008 455:1061. [PubMed: 18772890]

3. Yan H, Parsons DW, Jin GL, McLendon R, Rasheed BA, Yuan WS, Kos I, Batinic-Haberle I, Jones S, Riggins GJ, Friedman H, Friedman A, Reardon D, Herndon J, Kinzler KW, Velculescu VE, Vogelstein B, Bigner DD. New England Journal of Medicine. Feb.2009 360:765. [PubMed: 19228619]

4. Kloosterhof NK, Bralten LBC, Dubbink HJ, French PJ, van den Bent MJ. Lancet Oncology. Jan. 2011 12:83. [PubMed: 20615753]

5. Bleeker FE, Atai NA, Lamba S, Jonker A, Rijkeboer D, Bosch KS, Tigchelaar W, Troost D, Vandertop WP, Bardelli A, Van Noorden CJF. Acta Neuropathologica. Apr.2011 119:487. [PubMed: 20127344]

6. Mardis ER, Ding L, Dooling DJ, Larson DE, McLellan MD, Chen K, Koboldt DC, Fulton RS, Delehaunty KD, McGrath SD, Fulton LA, Locke DP, Magrini VJ, Abbott RM, Vickery TL, Reed JS, Robinson JS, Wylie T, Smith SM, Carmichael L, Eldred JM, Harris CC, Walker J, Peck JB, Du FY, Dukes AF, Sanderson GE, Brummett AM, Clark E, McMichael JF, Meyer RJ, Schindler JK, Pohl CS, Wallis JW, Shi XQ, Lin L, Schmidt H, Tang YZ, Haipek C, Wiechert ME, Ivy JV, Kalicki J, Elliott G, Ries RE, Payton JE, Westervelt P, Tomasson MH, Watson MA, Baty J, Heath S, Shannon WD, Nagarajan R, Link DC, Walter MJ, Graubert TA, DiPersio JF, Wilson RK, Ley TJ. New England Journal of Medicine. Sep.2009 361:1058. [PubMed: 19657110]

7. Dang L, White DW, Gross S, Bennett BD, Bittinger MA, Driggers EM, Fantin VR, Jang HG, Jin S, Keenan MC, Marks KM, Prins RM, Ward PS, Yen KE, Liau LM, Rabinowitz JD, Cantley LC, Thompson CB, Heiden MGV, Su SM. Nature. Dec.2009 462:739. [PubMed: 19935646]

8. Yen KE, Bittinger MA, Su SM, Fantin VR. Oncogene. Dec.2010 29:6409. [PubMed: 20972461]

9. Reitman ZJ, Jin GL, Karoly ED, Spasojevic I, Yang JA, Kinzler KW, He YP, Bigner DD, Vogelstein B, Yan H. Proceedings of the National Academy of Sciences of the United States of America. Feb.2011 108:3270. [PubMed: 21289278]

10. Sener RN. Journal of Computer Assisted Tomography. Jan-Feb;2003 27:38. [PubMed: 12544241]

11. Goffette SM, Duprez TP, Nassogne MCL, Vincent MFA, Jakobs C, Sindic CJ. European Journal of Neurology. May.2006 13:499. [PubMed: 16722976]

12. Provencher SW. Magnetic Resonance in Medicine. Dec.1993 30:672. [PubMed: 8139448]

13. Naressi A, Couturier C, Devos JM, Janssen M, Mangeat C, de Beer R, Graveron-Demilly D. Magnetic Resonance Materials in Physics Biology and Medicine. May.2001 12:141.

14. Mescher M, Merkle H, Kirsch J, Garwood M, Gruetter R. Nmr in Biomedicine. Oct.1998 11:266. [PubMed: 9802468]

15. Ernst RR. Chimia. 1975; 29:179.

16. Andronesi OC, Ramadan S, Mountford CE, Sorensen AG. Magnetic Resonance in Medicine. 2010; 64:1542. [PubMed: 20890988]

17. Bal D, Gryff-Keller A. Magnetic Resonance in Chemistry. Aug.2002 40:533.

18. Govindaraju V, Young K, Maudsley AA. Nmr in Biomedicine. May.2000 13:129. [PubMed: 10861994]

19. Opstad KS, Bell BA, Griffiths JR, Howe FA. Magnetic Resonance in Medicine. Nov.2008 60:1237. [PubMed: 18836999]

20. Ramadan S, Andronesi OC, Stanwell P, Lin AP, Sorensen AG, Mountford CE. Radiology. May. 2011 259:540. [PubMed: 21357517]

21. Usenius JP, Vainio P, Hernesniemi J, Kauppinen RA. Journal of Neurochemistry. Oct.1994 63:1538. [PubMed: 7931308]

22. Sabatier J, Gilard V, Malet-Martino M, Ranjeva JP, Terral C, Breil S, Delisle MB, Manelfe C, Tremoulet M, Berry I. Investigative Radiology. Mar.1999 34:230. [PubMed: 10084669]

23. Righi V, Roda JM, Paz J, Mucci A, Tugnoli V, Rodriguez-Tarduchy G, Barrios L, Schenetti L, Cerdan S, Garcia-Martin ML. Nmr in Biomedicine. Jul.2009 22:629. [PubMed: 19322812]

24. Beckonert O, Coen M, Keun HC, Wang YL, Ebbels TMD, Holmes E, Lindon JC, Nicholson JK. Nature Protocols. 5:1019.

25. Near J, Simpson R, Cowen P, Jezzard P. Nmr in Biomedicine. 2011 DOI: 10 1002/nbm.1688.

26. Kunz M, Thon N, Eigenbrod S, Hartmann C, Egensperger R, Herms J, Geisler J, la Fougere C, Lutz J, Linn J, Kreth S, von Deimling A, Tonn JC, Kretzschmar HA, Popperl G, Kreth FW. Neuro-Oncology. Mar.2011 13:307. [PubMed: 21292686]

27. Andronesi OC, Gagoski BA, Adalsteinsson E, Sorensen AG. NMR Biomedicine. 2011 doi: 10.1002/nbm.1730.

28. Zhu H, Edden RAE, Ouwerkerk R, Barker PB. Magnetic Resonance in Medicine. Mar.65:603.

29. Xu W, Yang H, Liu Y, Yang Y, Wang P, Kim SH, Ito S, Yang C, Wang P, Xiao MT, Liu LX, Jiang WQ, Liu J, Zhang JY, Wang B, Frye S, Zhang Y, Xu YH, Lei QY, Guan KL, Zhao SM, Xiong Y. Cancer Cell. Jan.2011 19:17. [PubMed: 21251613]

30. Williams SC, Karajannis MA, Chiriboga L, Golfinos JG, von Deimling A, Zagzag D. Acta Neuropathologica. Feb.2011 121:279. [PubMed: 21181477]

31. Kunz M, Thon N, Eigenbrod S, Hartmann C, Egensperger R, Herms J, Geisler J, la Fougere C, Lutz J, Linn J, Kreth S, von Deimling A, Tonn JC, Kretzschmar HA, Popperl G, Kreth FW. Neuro-Oncology. Mar.13:307. [PubMed: 21292686]

32. Dias-Santagata D, Akhavanfard S, David SS, Vernovsky K, Kuhlmann G, Boisvert SL, Stubbs H, McDermott U, Settleman J, Kwak EL, Clark JW, Isakoff SJ, Sequist LV, Engelman JA, Lynch TJ, Haber DA, Louis DN, Ellisen LW, Borger DR, Lafrate AJ. Embo Molecular Medicine. May.2010 2:146. [PubMed: 20432502]

33. Smith SA, Levante TO, Meier BH, Ernst RR. Journal of Magnetic Resonance Series A. Jan.1994 106:75.

34. Andronesi OC, Ramadan S, Ratai EM, Jennings D, Mountford CE, Sorensen AG. Journal of Magnetic Resonance. Apr.2010 203:283. [PubMed: 20163975]

One-sentence summary

2-Hydroxyglutarate, a metabolite overproduced in IDH-mutated gliomas, can be detected noninvasively in vivo in patients with brain tumors by optimized MRS methods.
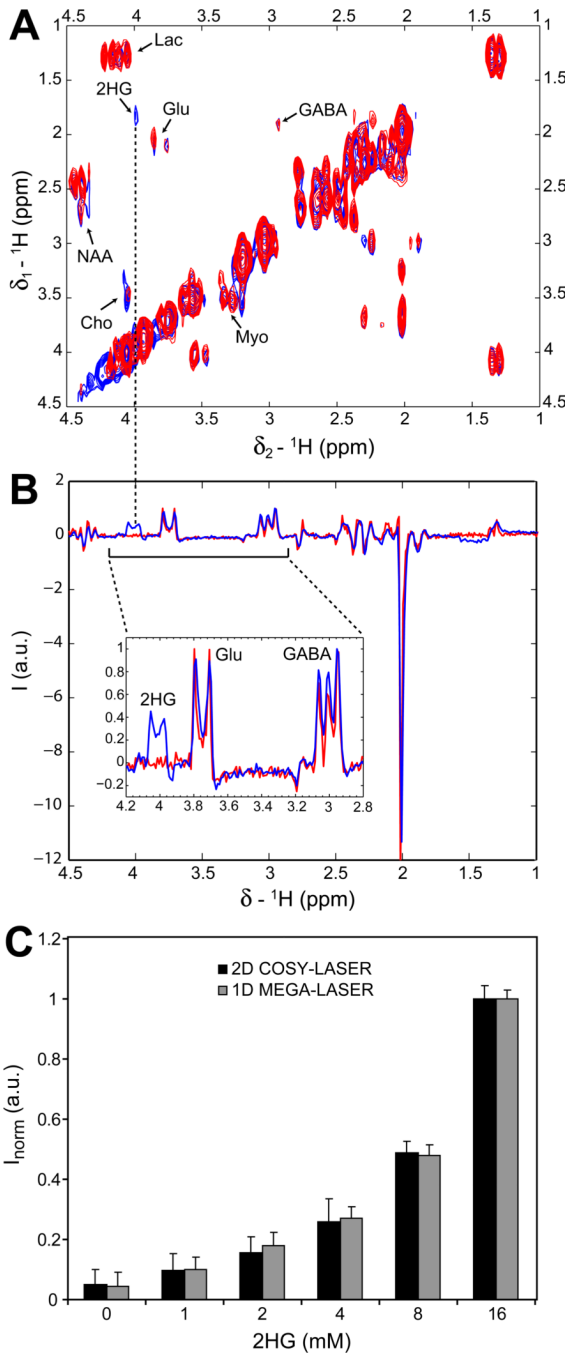
Fig. 1.
2D LASER-COSY and 1D MEGA-LASER spectra from brain phantoms at 3 T, with $3 \times 3 \times 3$ cm^3 voxels used in all measurements. (**A**) Overlay of 2D LASER-COSY spectra from a phantom containing a mixture of normal brain metabolites (red contours) and a phantom where 2HG was added to the mixture of normal brain metabolites (blue contours). The H$_\alpha$-H$_\beta$ crosspeak of 2HG is at 4.02/1.91 (δ_2/δ_1) ppm. (**B**) Overlay of 1D MEGA-LASER from the same phantoms. The position of Hα peak of 2HG at 4.02 ppm lines with the crosspeak in the 2D spectrum above (dashed line). (**C**) Intensity of 2HG signal in 2D LASER-COSY and 1D MEGA-LASER at different 2HG concentrations (error bars represent one standard deviation of two independent measures, signal intensity is normalized (I$_{norm}$) to the

maximum intensity). Other metabolites shown: choline (Cho), glutamate (Glu), lactate (Lac), myo-inositol (Myo), *N*-acetyl-aspartate (NAA).
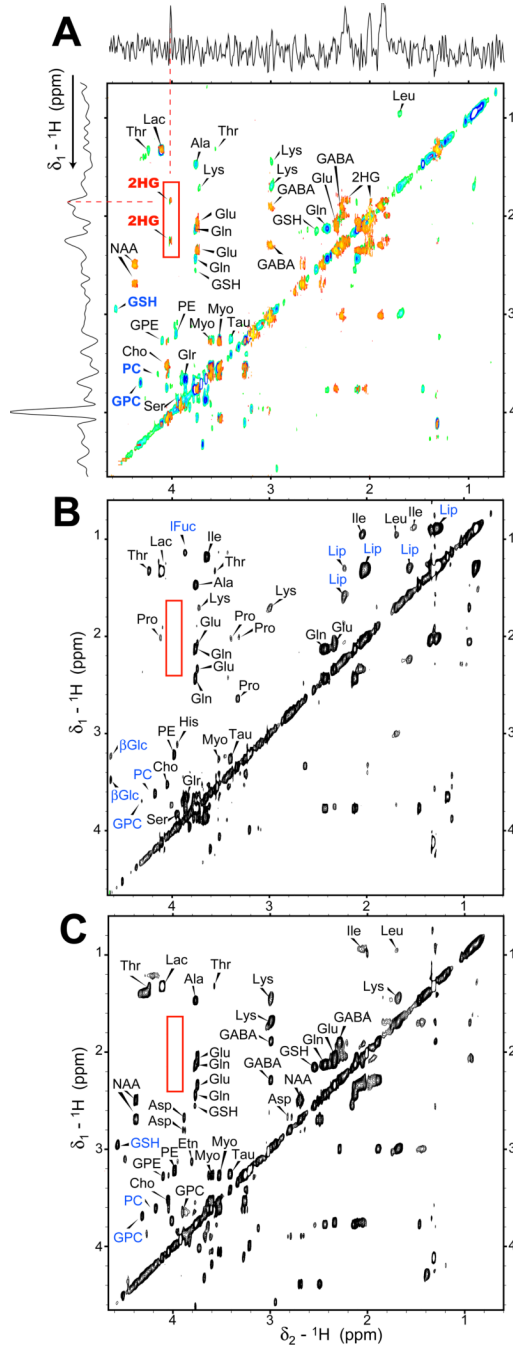
Fig. 2.
HR-MAS spectra recorded at 14 T ex vivo on biopsy tissue from patients with and without *IDH1* mutations. ^{1}H-^{1}H 2D TOBSY spectra are shown for all biopsies (the minimum contour levels were set five times the noise level). (**A**) For anaplastic astrocytoma biopsy tissue with $IDH1_{R132}$ mutation (*n*=1), the spectra are shown in green-blue contours. The phantom is shown in red-yellow. Projections along δ_1 and δ_2 show the 2HG crosspeaks, outlined by a red rectangle. (**B** and **C**) Spectra for wt-IDH1 patients: primary glioblastoma (B; *n*=1) and non-tumor (C; *n*=1). The region where 2HG crosspeaks would be expected is outlined by a red rectangle. For all 2D TOBSY brain spectra, several other metabolites can be identified. Amino acids: alanine (Ala), aspartate (Asp), glutamate (Glu), glutamine (Gln),

histidine (His), isoleucine (Ile), leucine (Leu), lysine (Lys), proline (Pro), serine (Ser), threonine (Thr). Membrane phospholipid-related compounds: choline (Cho), ethanolamine (Etn), glycerol (Glr), glycerophosphocholine (GPC), glycerophosphoethanolamine (GPE), phosphocholine (PC), phosphoethanolamine (PE). Sugars: l-fucose (lFuc), β-glucose (bGlc), myo-inositol (Myo). Miscellaneous: glutathione (GSH), lactate (Lac), lipids (Lip), *N*-acetyl-aspartate (NAA), and taurine (Tau).
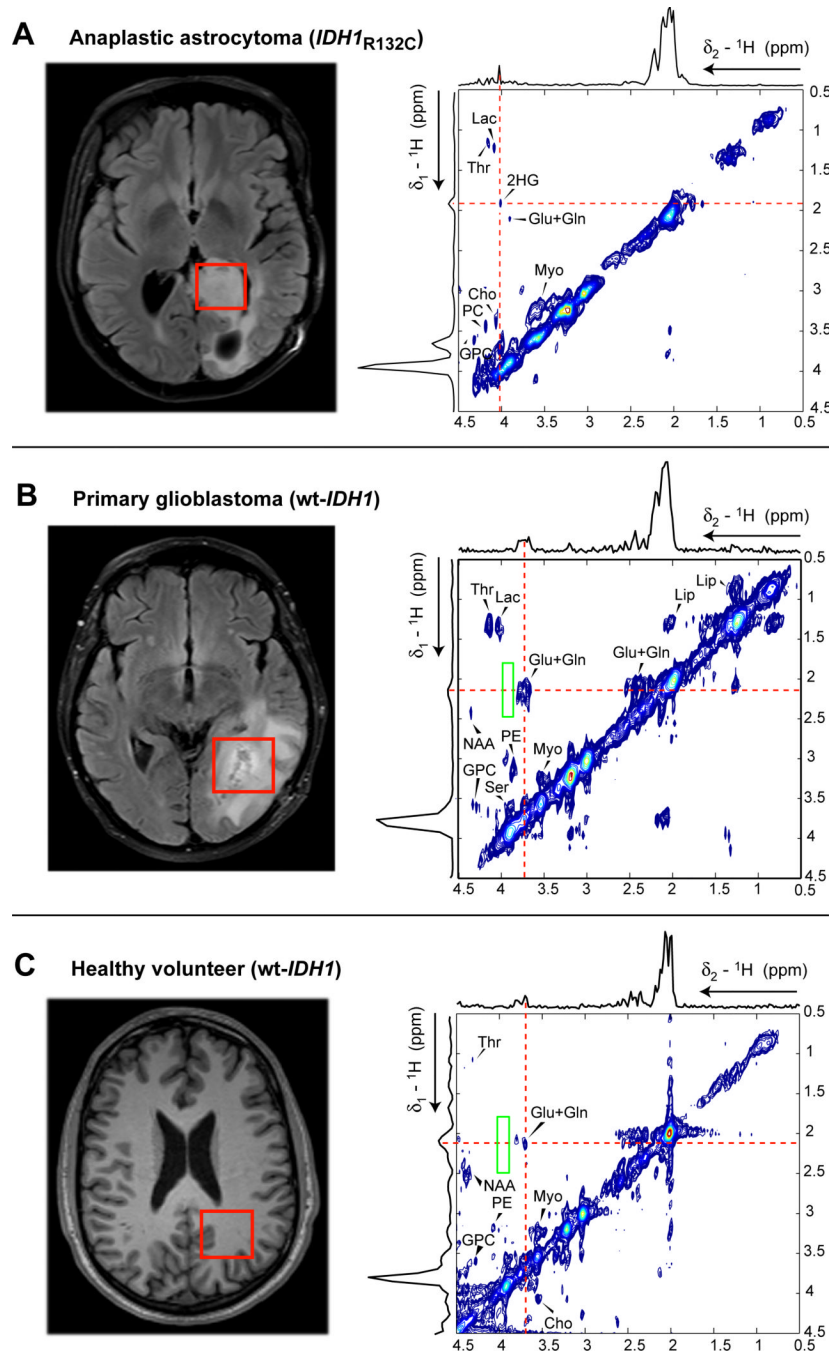
Fig. 3.
2D LASER-COSY spectra in human subjects at 3 T. (**A**) An anaplastic astrocytoma patient with $IDH1_{R132C}$. The 2D LASER-COSY shows at 4.02/1.91 ppm the H_α-H_β crosspeak of 2HG. Projections along both spectral dimensions through 2HG crosspeak indicate the SNR and spectral quality. The single voxel ($3 \times 3 \times 3$ cm^3, red rectangle) was placed on the FLAIR images to include most of the tumor abnormality. (**B**) A primary glioblastoma patient (wt-*IDH1*). The 2D LASER-COSY does not contain any 2HG crosspeak in the H_α-H_β region outlined by the green rectangle. Projections through Glu+Gln crosspeak indicate spectral quality. The single voxel ($3.5 \times 3.5 \times 3.5$ cm^3, red rectangle) was placed on the FLAIR images

to include most of the tumor abnormality. (**C**) A healthy volunteer (wt-*IDH1*). 2HG is not found in the H_α-H_β region of 2D LASER-COSY outlined by the green rectangle. Projections through Glu+Gln indicate spectral quality. The single voxel ($3\times3\times3$ cm^3, red rectangle) was placed on the MEMPRAGE images in the white matter of the occipital lobe, in a region similar to tumor locations from patients in (A) and (B).
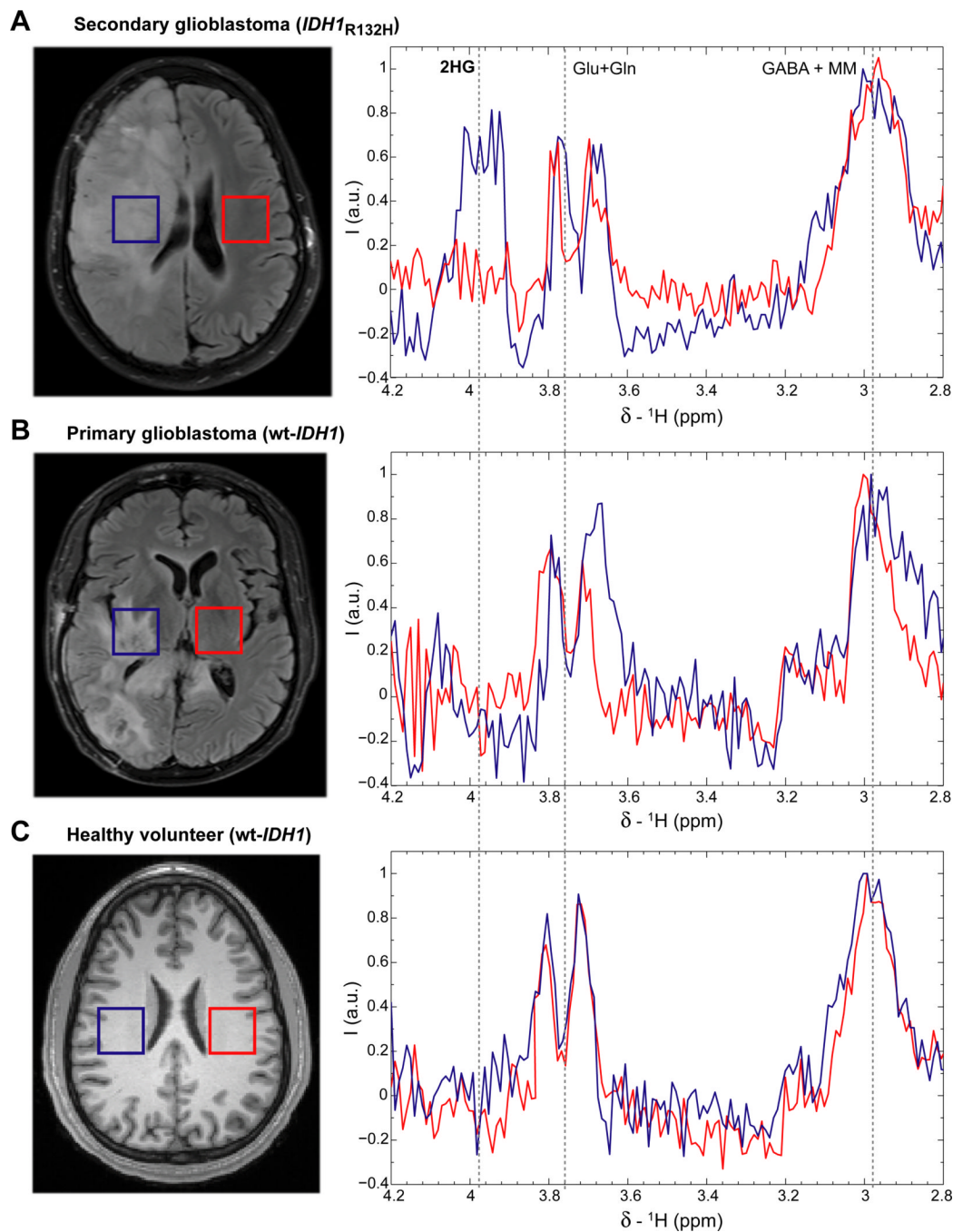
Fig. 4.
1D MEGA-LASER spectra in human subjects at 3 T. In all subjects two voxels ($3\times3\times3$ cm^3 each) were placed in both brain hemispheres, symmetrically from the middle line. (**A**) A secondary glioblastoma patient with $IDH1_{R132H}$ mutation. (**B** and **C**) The spectra from subjects with wt$IDH1$—primary glioblastoma (B) and healthy volunteer (C). 2HG is present only in the tumor voxel of $IDH1_{R132H}$ patient. (MM denotes contamination of GABA signal with macromolecule signal).
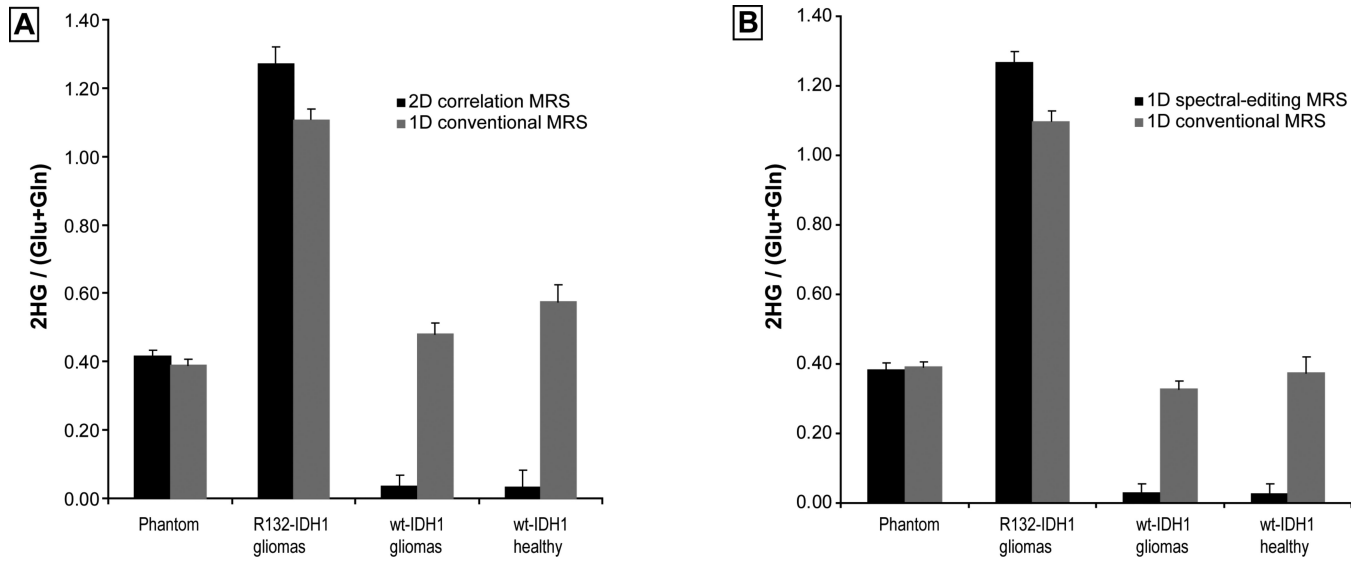
Fig. 5.
Signal intensity ratios of 2HG to the sum of glutamate and glutamine (Glu+Gln). (**A** and **B**) Ratios are shown for all phantom and in vivo human spectra: 2D correlation MRS (LASER-COSY) (**A**), 1D spectral-edited MRS (MEGA-LASER) (**B**), and 1D conventional MRS (LASER) (**A and B**). Ratios are given as averages +/− one standard deviation. $n = 2$ for phantoms and $IDH1_{R132}$ patients; $n = 4$ for wt-$IDH1$ subjects.

Table 1

Biopsies ($n = 10$) analyzed ex vivo with HR-MAS and LC-MS (bold letters indicate subjects showed in the figures).

Patient ID	Diagnosis	*IDH1* status	Age/Gender	Figures
1, 2	Anaplastic astrocytoma	**R132H,** wt	**54/M,** 31/F	**2A, S4**
3-7	Primary glioblastoma	wt	23/F, 40/F, 50/M, **52/M,** 52/F	**2B**
8-10	non-tumor	wt	8/M, 9/F, **17/M**	**2C**

Table 2

Human subjects ($n = 10$) scanned with in vivo MRS (bold letters indicate subjects showed in the figures).

Patient ID	Diagnosis	*IDH1* status	Age/Gender	Figures
1	Anaplastic astrocytoma	R132C	39/F	3A, S5
2	Secondary glioblastoma	R132H	41/F	4A, S8, S9
3-6	Primary glioblastoma	wt	70/F, **40/M,** 44/M, **52/F**	3B (52/F), S6 (52/F), 4B (40/M)
7-10	Healthy volunteer	wt	**30/F,** 34/M, 24/F, **32/M**	3C (30/F), S7 (30/F), 4C (32/M)